LIMNOLOGY
and
OCEANOGRAPHY

ASLO

*Limnol. Oceanogr.* 65, 2020, 13–26

doi: 10.1002/lno.11244

# Photodegradation disproportionately impacts biodegradation of semi-labile DOM in streams

**Jennifer C. Bowen**,[1] **Louis A. Kaplan**,[2] **Rose M. Cory**[1*]

[1]Earth and Environmental Sciences, University of Michigan, Ann Arbor, Michigan
[2]Stroud Water Research Center, Avondale, Pennsylvania

## *Abstract*

Exposure of dissolved organic matter (DOM) to sunlight can increase or decrease the fraction that is biodegradable (BDOM), but conceptual models fail to explain this dichotomy. We investigated the effect of sunlight exposure on BDOM, addressing three knowledge gaps: (1) how fractions of DOM overlap in their susceptibility to degradation by sunlight and microbes, (2) how the net effect of sunlight on BDOM changes with photon dose, and (3) how rates of DOM photodegradation and biodegradation compare in a stream. Stream waters were exposed to sunlight, and then fed through bioreactors designed to separate labile and semi-labile pools within BDOM. The net effects of photodegradation on DOM biodegradability, while generally positive, represented the balance between photochemical production and removal of BDOM that was mediated by photon dose. By using sunlight exposure times representative of sunlight exposures in a headwater stream and bioreactors colonized with natural communities and scaled to whole-stream dynamics, we were able to relate our laboratory findings to the stream. The impact of sunlight exposure on rates of DOM biodegradation in streams was calculated using rates of light absorption by chromophoric DOM, apparent quantum yields for photomineralization and photochemical alteration of BDOM, and mass transfer coefficients for labile and semi-labile DOM. Rates of photochemical alteration of labile DOM were an order of magnitude lower than rates of biodegradation of labile DOM, but for semi-labile DOM, these rates were similar, suggesting that sunlight plays a substantial role in the fate of semi-labile DOM in streams.

Terrestrially derived dissolved organic matter (DOM) sourced from decaying plant and soil organic matter fuels heterotrophic microbial degradation in streams (Battin et al. 2008). Export of terrestrially derived DOM to streams in many regions has increased in response to changes in climate, land-use, or other processes (Monteith et al. 2007; Laudon et al. 2009; Singh et al. 2016). However, controls on the biodegradation of DOM to $CO_2$ remain too poorly understood to predict changes in $CO_2$ emissions from streams in response to increasing DOM export from watersheds (Oni et al. 2015; Biddanda 2017).

Following export of terrestrially derived DOM to sunlit streams, photodegradation of DOM may be a major control on its biodegradation (Cory and Kling 2018). In sunlit waters, the chromophoric fraction of DOM (CDOM) absorbs sunlight, initiating photochemical reactions that can photomineralize DOM to $CO_2$ (Granéli et al. 1996; Lindell et al. 2000) or photo-alter the chemical composition of DOM by producing different DOM compounds (Cory et al. 2007; Gonsoir et al. 2009; Ward and Cory 2016). Evidence suggests that some of the DOM compounds that are photomineralized or photo-altered are also biodegradable (BDOM; Moran et al. 2000; Cory et al. 2010*a*; Amado et al. 2015; Ward et al. 2017). This potential overlap between photo- and biodegradation of DOM creates a range of scenarios in which sunlight and microbes may both cooperate and compete to degrade DOM. Sunlight and microbes cooperate to degrade DOM when sunlight photo-alters relatively recalcitrant, high-molecular weight (HMW) DOM to produce biodegradable low-molecular weight (LMW) acids or aldehydes (Wetzel et al. 1995; Bertilsson and Tranvik 1998). On the other hand, sunlight and microbes compete to degrade DOM when sunlight photomineralizes BDOM, or photo-alters BDOM to compounds no longer biodegradable (Cory et al. 2010*a*; Ward et al. 2017).

The presence of these cooperative and competitive interactions, as well as the balance between them, may help reconcile widespread observations of both positive and negative effects of sunlight on DOM biodegradability (Tranvik and Bertilsson 2001; Amado et al. 2007). However, we cannot predict the net effect of sunlight on DOM biodegradability because the fractions of DOM accounting for increases and decreases in BDOM on a mass basis are not well known. For example, photochemical production of compounds thought to contribute to increased BDOM, such as acetate and amino acids, can only account for

*Correspondence: rmcory@umich.edu

Additional Supporting Information may be found in the online version of this article.

small changes in BDOM on a mass basis following photodegradation of terrestrially derived DOM (Wetzel et al. 1995; Bertilsson and Tranvik 1998; Pullin et al. 2004). Likewise, fractions of DOM removed by sunlight are not well constrained on a mass basis, but may include a range of aliphatic (Ward et al. 2017), aromatic (Cory et al. 2010*a*), and nitrogen-rich protein-like DOM (Amado et al. 2015).

The photochemical production and removal of BDOM that account for cooperative and competitive interactions between sunlight and microbes to degrade DOM may be inferred by examining changes in CDOM and the fluorescent fraction of DOM (FDOM) following photo- and biodegradation (Moran et al. 2000; Obernosterer and Benner 2004; Fasching and Battin 2012; Amado et al. 2015). CDOM and FDOM are proxies for sources and compositions of carbon within the DOM pool, such as HMW, aromatic carbon associated with terrestrially derived DOM or carbon associated with free or combined fluorescent amino acids (e.g., tryptophan, tyrosine, and phenylalanine; Coble 1996). CDOM and FDOM are fractions of DOM most susceptible to photodegradation (Lindell et al. 2000; Moran et al. 2000) and that are also biodegradable (Guillemette and del Giorgio 2011; Cory and Kaplan 2012). Thus, many studies have made inferences on cooperative and competitive interactions between sunlight and microbes to degrade DOM by analyzing the overlap (or lack thereof) between CDOM and FDOM degraded by sunlight or microbes alone (Moran et al. 2000; Obernosterer and Benner 2004; Fasching and Battin 2012; Amado et al. 2015). However, what is missing from these studies, but needed to quantify how sunlight impacts biodegradation of DOM in streams, is the connection between the fractions of DOM degraded by sunlight and microbes and the rates of each process, photo- and biodegradation, in streams.

The few studies that have directly compared rates of DOM photo- and biodegradation in streams have showed that photodegradation can be as fast as or faster than biodegradation of DOM in the water column (Cory et al. 2014, 2015). However, it is not known how rates of DOM photodegradation compare to rates of biodegradation of DOM in the benthic zone of the streambed, the habitat where most microbial activity occurs in streams. For example, the DOM fractions accounting for increases or decreases in BDOM after sunlight exposure on a mass basis may not impact organic matter processing in streams if rates of their photochemical production or removal are too slow compared to rates of their biodegradation in the streambed. Thus, knowing how sunlight impacts DOM biodegradability in a stream reach requires a comparison of the rates of photodegradation of DOM fractions in the water column to rates of their biodegradation in the streambed.

The balance of photochemical production and removal of BDOM, and thus the net effect of sunlight on DOM biodegradability, should depend strongly on the amount of light received by DOM as it travels downstream. This is because the extent of DOM photodegradation increases as CDOM absorbs more light with increasing photon dose (Granéli et al. 1996; Lindell et al. 2000; Moran et al. 2000). The only study that has quantified the effect of photon dose on DOM biodegradability showed diminished enhancement of DOM biodegradability with increasing photon dose (Reader and Miller 2014). Those findings have been interpreted to mean that photochemical production of BDOM becomes increasingly offset by the removal of BDOM with increasing photon dose. However, in that study, waters were exposed to high doses of light comparable to sunlight exposures in coastal waters not streams (Reader and Miller 2014). Quantifying the net effect of sunlight on DOM biodegradability following photon doses representative of those in streams is thus needed to determine the effects of photon dose on stream water DOM biodegradability and estimate rates of DOM photodegradation in streams.

Here, we address three knowledge gaps on the effect of sunlight exposure on BDOM: (1) how fractions of DOM overlap in their susceptibility to degradation by sunlight and microbes, (2) how the net effect of sunlight on BDOM changes with photon dose, and (3) how rates of photodegradation and biodegradation of DOM compare in a stream. Stream water was exposed to sunlight alongside dark controls to mimic sunlight exposure times in streams and then fed through bioreactors designed to separate labile and semi-labile pools within BDOM. We evaluated overlap between CDOM and FDOM fractions that were photo- and biodegraded to qualitatively interpret changes in BDOM following photodegradation. By using short-term sunlight exposure times representative of sunlight exposures in streams and short-term biodegradation experiments with bioreactors colonized with natural communities and scaled to whole-stream dynamics, we related our laboratory findings to in situ rates in the stream reach. Photodegradation rates were calculated using light absorption by CDOM throughout the stream water column and apparent quantum yields (AQYs) for photomineralization and for photochemical alteration of labile or semi-labile DOM. Biodegradation rates were calculated using prior instream measures of mass transfer coefficients for labile and semi-labile DOM. The net effect of photodegradation on DOM biodegradability was generally positive and resulted from the photo-alteration of DOM to produce and remove BDOM. Photon dose impacted photochemical production and removal of BDOM, and in doing so, impacted the net effect of sunlight on the biodegradability of DOM. Finally, rates of photochemical alteration of labile DOM (i.e., net production or removal) were much lower than rates of biodegradation of labile DOM, but were similar for semi-labile DOM, suggesting that sunlight may be particularly important in controlling the fate of the semi-labile DOM pool in stream ecosystems.

## Methods

### Experimental design

#### *Site description and sampling*

A total of five stream water samples were collected from a third-order reach of White Clay Creek (WCC; 39°51′N, 75°47′W)

in persulfate-cleaned 20-liter carboys during August 2016 and May 2017 (Table 1). This temperate stream in the southeastern Pennsylvania Piedmont flows through intact riparian woodlands (Newbold et al. 1997). All stream waters were collected at 06:00 h, within 0.5 h of sunrise, with four collected under baseflow conditions and one collected on the receding limb of a storm hydrograph. Stream waters were filtered immediately in a two-step process using organic-C free GF/F filters followed by sterile, 0.2 $\mu$m filters (Pall Corporation), and stored at 4°C in a separate, persulfate-cleaned carboy in the dark for ≤ 9 d before a sunlight exposure experiment.

### *Sunlight exposure of DOM*

Aliquots of each filtered stream water sample were used in 1–4 separate sunlight exposures ranging from 3 to 17 h (Table 1). Sunlight exposures were performed by equilibrating 2 L of a sample to room temperature, distributing 1 L into 10 precombusted (450°C, 5 h) 100-mL quartz tubes with ground glass stoppers, and exposing the tubes to natural sunlight on a black surface alongside a dark control kept in a foil-wrapped, precombusted 1-liter borosilicate glass bottle (Supporting Information Fig. S1). Exposures took place on cloudy and sunny days, during which the temperature of waters in the quartz tubes ranged from 27°C to 32°C compared to 25°C to 26°C in the dark controls. Following sunlight exposure, waters from the quartz tubes were composited into a precombusted 1-liter borosilicate glass bottle (Supporting Information Fig. S1), and both the light-exposed and dark control samples were stored in the dark at 4°C for < 1 d until bioreactor experiments. In total, 15 sunlight exposure experiments took place on separate days, generating 15 sets of light-exposed and dark control samples (Table 1).

### *Bioreactor approach to quantify BDOM*

Plug-flow biofilm reactors (i.e., bioreactors) are chromatography columns filled with sintered glass beads that are maintained by continuous inputs of WCC waters that are filtered to remove larger particles but allow suspended bacteria to pass. Over time, the bioreactors, covered to eliminate light and maintained in a room kept at 20°C, were colonized and fed by a unidirectional flow of WCC water and suspended bacteria which generated gradients of bacterial densities, species composition, and activity (Kaplan and Newbold 1995). Bioreactors were constructed with different volumes to vary the empty bed contact times (EBCT), or the amount of time that BDOM is available for uptake, such that EBCT could be used as a surrogate for the relative biodegradability of DOM. For example, the most biologically labile compounds are rapidly degraded over short bioreactor contact times and semi-labile compounds are degraded following longer contact times (Kaplan et al. 2008). Bioreactors facilitate the measurements of BDOM without the confounding issues of groundwater and tributary inputs, disturbances from elevated storm flows, phototrophs, and seasonal and diel temperature variations. Prior work comparing the behavior of a $^{13}$C-DOC tracer in bioreactors and in WCC scaled DOM biodegradation in the bioreactors to the stream, where the uptake of BDOM occurring in the bioreactors over minutes and centimeters occurred in the stream over hours to days and hundreds of meters to kilometers (Kaplan et al. 2008).

We used bioreactors to quantify BDOM in the light-exposed or dark control water samples (Kaplan and Newbold 1995; Cory and Kaplan 2012) and to separate the BDOM into operationally defined labile and semi-labile pools (Kaplan et al. 2008). Samples

**Table 1.** Summary of the sunlight exposure and biodegradation experiments conducted with WCC water. Biodegradation experiments were conducted using two bioreactors with different EBCT.

| Date of collection | Sunlight exposure in quartz tubes (h) | Photon dose (mol photon $m^{-2}$) | Light absorbed by CDOM (mol photon $m^{-2}$) | Equivalent sunlight exposure in WCC (h) | Bioreactor EBCT (min) |
|---|---|---|---|---|---|
| 14 Aug 2016 | 10 | 24 | 0.22 | 2.0 | 37 |
| | 12 | 26 | 0.25 | 2.2 | 1.5 |
| | 12 | 28 | 0.29 | 2.5 | 37 |
| 20 May 2017 | 5 | 5 | 0.08 | 0.9 | 37 |
| | 9 | 7 | 0.11 | 1.2 | 1.5 |
| | 10 | 9 | 0.14 | 1.6 | 37 |
| | 12 | 17 | 0.21 | 2.3 | 37 |
| 21 May 2017 | 5 | 2 | 0.03 | 0.4 | 37 |
| | 6 | 8 | 0.09 | 1.2 | 1.5 |
| | 11 | 18 | 0.17 | 2.5 | 37 |
| | 12 | 22 | 0.22 | 3.2 | 37 |
| 27 May 2017* | 3 | 2 | 0.06 | 0.4 | 37 |
| | 4 | 3 | 0.08 | 0.5 | 37 |
| | 8 | 9 | 0.24 | 1.5 | 37 |
| 28 May 2017 | 17† | 29 | 0.29 | 3.8 | 37 |

*Stream water collected 24 h after a storm (41 mm of precipitation).
†Stream water was exposed to natural sunlight over a period of 2 d.

were individually fed through a bioreactor with an EBCT of either 1.5 or 37 min, and the bioreactor influent and effluent waters were collected in triplicate in precombusted borosilicate glass vials for dissolved organic carbon (DOC), CDOM, and FDOM analyses (Supporting Information Fig. S1). The bioreactor with an EBCT of 1.5 min was used to quantify the labile pool within BDOM and the bioreactor with an EBCT of 37 min was used to quantify total BDOM, which includes both the labile and semi-labile pools (Kaplan et al. 2008). Of the 15 sets of light-exposed and dark control samples, three were used to quantify only the labile pool and 12 were used to quantify total BDOM (Table 1).

Prior studies have quantified total BDOM using a bioreactor with an EBCT of 150 min (Kaplan et al. 2008; Sleighter et al. 2014). As such, BDOM quantified in the 37-min EBCT bioreactor, used here because of volume constraints associated with the quartz tubes, underestimates total BDOM by approximately 20% (*see* Supporting Information). For simplicity of presentation, hereafter we refer to the data from the 37-min EBCT bioreactor as total BDOM (Supporting Information Table S1).

**DOC, CDOM, and FDOM analyses**

DOC samples were refrigerated at 4°C and analyzed within < 1 d of collection. CDOM and FDOM samples were made biologically stable by a modification of the Tyndallization procedure (Tyndall 1877) involving three cycles of heating in a water bath to 60°C for 5 min, followed by 30 min at 25°C (Kaplan et al. unpubl.); samples were analyzed within < 3 weeks of Tyndallization. DOC concentrations were measured by UV-catalyzed persulfate oxidation with conductimetric detection (Sievers 900 analyzer). Optical properties of CDOM were analyzed using a UV-Vis spectrophotometer with a 10-cm (Cary Varian 300) or 1-cm pathlength cuvette (Aqualog, Horiba) against laboratory-grade deionized water blanks. CDOM absorption coefficients were calculated as follows:

$$a_{\mathrm{CDOM},\lambda} = \frac{A_\lambda}{l} 2.303 \quad (1)$$

where $A$ is the absorbance at wavelength $\lambda$ and $l$ is the pathlength in meters.

The specific UV absorbance at 254 nm ($SUVA_{254}$), a proxy for aromatic content of DOM, was calculated as the absorbance at 254 nm divided by the pathlength (m) and by the concentration of DOC (mg C $L^{-1}$; Weishaar et al. 2003). The spectral slope ratio ($S_R$), a proxy for the molecular weight of DOM, was calculated from the CDOM absorbance spectrum following Helms et al. (2008).

Excitation emission matrices (EEMs) were measured using an Aqualog fluorometer (Horiba). EEMs were collected across excitation wavelengths 240–450 nm with 5 nm increments and emission wavelengths 320–550 nm with 2 nm increments using integration times of 4 or 5 s. EEMs were corrected for inner-filter effects and for instrument-specific excitation and emission corrections in MATLAB (version 8.5) as previously described (Cory et al. 2010*b*; Cory and Kaplan 2012). EEMs of laboratory-grade deionized water blanks were subtracted from the sample EEMs and the fluorescence intensities were converted to Raman units (RU; Stedmon and Bro 2008).

Parallel factor analysis (PARAFAC) was used to separate a data set of EEMs of WCC water into mathematically and chemically independent components, as previously described (Cory and Kaplan 2012). Briefly, all five FDOM components in WCC water were validated by PARAFAC analysis (Cory and Kaplan 2012). The humic-like C2 and C3 correspond to peaks A and C, respectively (Coble 1996), which have been associated with terrestrially derived material, such as products of lignin degradation (Del Vecchio and Blough 2004; Hernes et al. 2009) and aromatic carbon content of DOM (Cory and McKnight 2005; Cory et al. 2007). The humic-like C1 has been associated with recent autochthonous production (peak M; Murphy et al. 2008). The amino acid-like C4 and C5 overlap with the fluorescence of the amino acids tryptophan and tyrosine, respectively (Cory and McKnight 2005; Stedmon and Markager 2005), and their fluorescence has been shown to increase with the percentage of protein-like compounds within the DOM pool in WCC water (Sleighter et al. 2014). The $F_{max}$ value of each component was quantified to estimate its relative abundance within an EEM (in RU; Cory and Kaplan 2012).

**Calculations**

***Amount of light absorbed by CDOM***

The photon dose (mol photon $m^{-2}$) during each light exposure period was calculated from measurements of the global solar irradiance spectra at WCC. That spectrum, including direct and diffuse irradiance, was measured approximately hourly with a radiometer over wavelengths from 280 to 600 nm (USB4000 Spectrometer, Ocean Optics). Every global solar irradiance spectrum ($\mu$W $cm^{-1}$ $nm^{-1}$) was converted to a photon flux spectrum (mol photon $m^{-2}$ $s^{-1}$ $nm^{-1}$) assuming that the photon flux spectra during each time interval were equal to the average photon flux spectrum bracketed by two consecutive measurements. The average photon flux spectrum between any two consecutive measurements was multiplied by the duration of the time interval to calculate the photon flux spectrum for that interval (mol photon $m^{-2}$ $nm^{-1}$). The photon flux spectra during each time interval were summed to calculate the total photon flux spectrum during the light exposure period ($E_{0,\lambda}$; mol photon $m^{-2}$ $nm^{-1}$), and across all wavelengths to calculate the photon dose.

The extent of DOM photodegradation depends on the amount of light absorbed by CDOM, which is a product of photon dose and the concentration of CDOM available to absorb the light. Thus, we calculated the amount of light absorbed by CDOM during each light exposure period ($Q_{a,\lambda}$; mol photons $m^{-2}$) as follows:

$$Q_{\mathrm{a},\lambda} = \int_{\lambda_{\min}}^{\lambda_{\max}} E_{0,\lambda}\left(1 - \mathrm{e}^{-a_{\mathrm{CDOM},\lambda} \times z}\right) \frac{a_{\mathrm{CDOM},\lambda}}{a_{\mathrm{tot},\lambda}} d\lambda \quad (2)$$

where $\lambda_{min}$ and $\lambda_{max}$ are the minimum and maximum wavelengths of light absorbed by CDOM (280 nm and 600 nm, respectively). $E_{0,\lambda}$ is the total photon flux spectrum during the light exposure period (mol photon $m^{-2}$ $nm^{-1}$). We assumed that the pathlength of light ($z$) was equivalent to the diameter of the quartz tubes (3 cm) and that the fraction of light absorbed by CDOM relative to other light-absorbing constituents, $a_{CDOM,\lambda}/a_{tot,\lambda}$, was equal to 1 at all wavelengths in the filtered stream water (Cory et al. 2014).

### *Concentration vs. composition of DOM and BDOM*

Our approach to understand the impact of sunlight exposure on DOM biodegradability involves the quantification of different operationally defined fractions of DOM (Supporting Information Table S1). We use DOC and biodegradable DOC (BDOC) for carbon concentrations of DOM amenable to mass balance analyses, and CDOM, FDOM, and BDOM for compositions of chromophoric, fluorescent, and biodegradable fractions (BDOM), respectively, that are not quantifiable on a mass basis. The expected relationships and overlap among these operational fractions of DOM, including CDOM, FDOM, and BDOM, are shown in Supporting Information Fig. S2.

Photomineralization was quantified as the difference in DOC concentrations between the light-exposed and dark control samples. Photodegradation of DOM was quantified as the light-exposed minus dark control difference in CDOM and FDOM (Supporting Information Table S1). BDOC concentration and BDOM composition were quantified as differences in DOC concentration and CDOM or FDOM between the influent and effluent waters from a bioreactor (Supporting Information Table S1; Kaplan et al. 2008; Cory and Kaplan 2012). The effects of sunlight exposure on DOM biodegradation were calculated as differences between BDOC concentrations or BDOM compositions in the light-exposed waters and the respective dark controls.

For the purpose of calculating rates of biodegradation in the stream, concentrations of labile and semi-labile DOC were estimated from the total BDOC concentration (Supporting Information Table S2) based on prior work showing that 39% of the BDOC concentration degraded within a 37-min EBCT was in the labile pool, with the remaining 61% of BDOC in the semi-labile pool (*see* Supporting Information). Thus, concentrations of labile DOC were both quantified using the 1.5-min EBCT bioreactor ($n$ = 3) and estimated as a percentage of total BDOC degraded in the 37-min EBCT bioreactor ($n$ = 12), whereas concentrations of semi-labile DOC were only estimated as a percentage of total BDOC ($n$ = 12).

### *Sunlight exposure times in the stream*

Sunlight exposure times in the quartz tubes were converted to sunlight exposure times in WCC by a two-step process. First, we calculated hourly water column rates of light absorption by CDOM in WCC (Eq. 2) using 0.145 m as the average depth of WCC (based on 29 separate salt injections; J. D. Newbold unpubl.), the initial CDOM in the stream water (Table 2), and the average hourly incoming photon flux spectrum (mol photon $m^{-2}$ $h^{-1}$ $nm^{-1}$) measured on each date of stream water collection. Second, the amount of light absorbed by CDOM in the quartz tubes during each light exposure period (mol photons $m^{-2}$) was divided by the hourly water column rate (mol photons $m^{-2}$ $h^{-1}$) to calculate the sunlight exposure time in the stream (Table 1).

### *Rates of photo- and biodegradation of DOM in the stream*

We compared rates of DOM biodegradation in the streambed of WCC to rates of photodegradation in the water column of WCC on a mass basis. Areal rates of biodegradation (mg C $m^{-2}$ $d^{-1}$) of labile and semi-labile DOC in the streambed were calculated by multiplying mass transfer coefficients ($\mu$m $s^{-1}$), previously determined for labile and semi-labile DOC pools in WCC (Kaplan et al. 2008), by the concentrations of labile and semi-labile DOC in the dark control waters in this study, respectively ($n$ = 15 and 12; discussed above).

Areal rates of DOM photodegradation (mg C $m^{-2}$ $d^{-1}$) are the product of two spectra: the rate of light absorption by CDOM throughout the water column in WCC ($Q_{a,\lambda}$) and the AQY ($\Phi_\lambda$):

$$\text{Rate of DOM photodegradation} = \int_{\lambda_{min}}^{\lambda_{max}} Q_{a,\lambda}\Phi_\lambda d\lambda \qquad (3)$$

**Table 2.** Average concentrations of DOM fractions in WCC water. Letters indicate significant differences (ANOVA, $p < 0.05$) among stream waters. All values listed as average ± 1 SE of triplicate measurements.

| | Date of collection | | | | |
|---|---|---|---|---|---|
| **DOM fraction** | **14 Aug 2016** | **20 May 2017** | **21 May 2017** | **27 May 2017** | **28 May 2017** |
| DOC (mg C $L^{-1}$) | $1.46 \pm 0.01^{a}$ | $1.74 \pm 0.01^{c}$ | $1.43 \pm 0.01^{a}$ | $2.39 \pm 0.01^{d}$ | $1.69 \pm 0.01^{b}$ |
| $a_{305}$ ($m^{-1}$) | $5.77 \pm 0.08^{b}$ | $5.59 \pm 0.01^{b}$ | $4.71 \pm 0.03^{a}$ | $9.35 \pm 0.01^{d}$ | $6.05 \pm 0.01^{c}$ |
| $SUVA_{254}$ (L mg $C^{-1}$ $m^{-1}$) | $2.95 \pm 0.02^{c}$ | $2.56 \pm 0.02^{a}$ | $2.43 \pm 0.03^{a}$ | $2.99 \pm 0.01^{c}$ | $2.75 \pm 0.01^{b}$ |
| $S_R$ | $0.68 \pm 0.02^{ab}$ | $0.74 \pm 0.01^{c}$ | $0.69 \pm 0.01^{a}$ | $0.71 \pm 0.01^{b}$ | $0.70 \pm 0.01^{ab}$ |
| Humic-like C1 (RU) | $0.41 \pm 0.01^{b}$ | $0.41 \pm 0.01^{b}$ | $0.36 \pm 0.01^{a}$ | $0.68 \pm 0.01^{d}$ | $0.49 \pm 0.01^{c}$ |
| Tryptophan-like C4 (RU) | $0.13 \pm 0.01^{b}$ | $0.13 \pm 0.01^{b}$ | $0.11 \pm 0.01^{a}$ | $0.21 \pm 0.01^{d}$ | $0.16 \pm 0.01^{c}$ |
| Tyrosine-like C5 (RU) | $0.05 \pm 0.01^{a}$ | $0.06 \pm 0.01^{b}$ | $0.05 \pm 0.01^{a}$ | $0.08 \pm 0.01^{c}$ | $0.06 \pm 0.01^{b}$ |

The AQY is a measure of the susceptibility of DOM to photodegradation defined as the moles of product formed per mole of photons absorbed by CDOM at each wavelength. For example, the AQY for photomineralization was calculated as the light minus dark difference in DOC concentration divided by the light absorbed by CDOM during the light exposure period that resulted in detectable loss of DOC in each stream water sample ($n$ = 5; Supporting Information Table S2), assuming the AQY spectra decreased exponentially with increasing wavelength (Vähätalo et al. 2000; Cory et al. 2013, 2014; Cory and Kling 2018). Daily water column rates of light absorption by CDOM were calculated as described above (Eq. 2) using the average depth of WCC (0.145 m), the initial CDOM in the stream water (Table 2), and the daily incoming photon flux spectrum (mol photon $m^{-2}$ $d^{-1}$ $nm^{-1}$) measured on each date of stream water collection.

Quantifying areal rates of DOM photodegradation on a mass basis (mg C $m^{-2}$ $d^{-1}$) is limited to processes that form a product quantified on a per carbon basis. Because the products of DOM photo-alteration are not well known or quantifiable on a per carbon basis (e.g., photobleaching that leads to removal of CDOM and FDOM), we used two conservative assumptions to quantify AQYs on a mass basis for photochemical production and removal of BDOM. First, we used the light minus dark difference in BDOC concentration (Supporting Information Table S2) to quantify the net effect of DOM photodegradation on BDOM. Second, we assumed that the AQY spectra for photochemical production and removal of BDOM decreased exponentially with increasing wavelength (Vähätalo et al. 2000; Cory et al. 2013, 2014; Cory and Kling 2018). AQYs for the photo-production of BDOM were calculated for waters that showed a net increase in BDOC concentration (e.g., 0.03–0.12 mg C $L^{-1}$ BDOC produced after 0.08–0.28 mol photon $m^{-2}$ of light was absorbed by CDOM; Fig. 4, Supporting Information Table S2; labile DOC ($n$ = 3) and total BDOC ($n$ = 6)). AQYs for the photo-removal of BDOM were calculated for waters that showed a net decrease in BDOC concentration (e.g., 0.05–0.14 mg C $L^{-1}$ BDOC removed after 0.22–0.29 mol photon $m^{-2}$ of light was absorbed by CDOM; Fig. 4, Supporting Information Table S2; total BDOC ($n$ = 6)). Rates of photochemical production or removal of total BDOC were separated into labile and semi-labile pools assuming that 39% and 61% of the total BDOC photo-produced or photo-removed were labile and semi-labile, respectively.

### *Statistical analyses*

DOC, CDOM, and FDOM are reported as the average value ± 1 standard error (SE) of the triplicate measurements (Supporting Information Fig. S1), unless otherwise noted. DOC, CDOM, and FDOM were compared among the five stream waters collected using ANOVA. Paired $t$-tests were used to determine significant differences between percentages of photodegraded DOM and total BDOM in the dark control, and between percentages of total BDOM in the light-exposed and dark control waters. Statistical significance was defined as $p < 0.05$.

## *Results*

Stream waters collected for the sunlight exposure experiments exhibited a range of DOC, CDOM, and FDOM concentrations, with the greatest differences driven by hydrology. The stream water sample collected on 27 May, as the stream hydrograph receded from a storm 24 h earlier that had increased discharge by approximately 15-fold over baseflow, was distinguished by concentrations of DOM fractions that were 40–70% greater than the average for the four stream waters collected under baseflow conditions (Table 2). In contrast, under baseflow conditions, the average concentrations of DOM fractions varied by < 15% and averaged as follows (average ± SE): DOC, 1.58 ± 0.16 mg C $L^{-1}$; $a_{305}$, 5.53 ± 0.58 $m^{-1}$; humic-like C1, 0.42 ± 0.05 RU; tryptophan-like C4, 0.13 ± 0.02 RU; and tyrosine-like C5, 0.05 ± 0.01 RU ($n$ = 4; Table 2). DOM compositions as measured by $SUVA_{254}$ and $S_R$ were similar across all five stream waters collected (Table 3).

Sunlight exposures of the quartz tubes ranged from 3 to 17 h, which were equivalent to exposure times of 0.4–3.8 h in the stream water column (Table 1). During the sunlight exposure experiments, the extent of DOM photodegradation increased as the amount of light absorbed by CDOM increased over a range of 0.03–0.29 mol photon $m^{-2}$ (Fig. 1), or over photon doses ranging from 2 to 29 mol photon $m^{-2}$ (Supporting Information Fig. S3). Increased photodegradation with light absorption was linear for DOC and the DOM fractions $a_{305}$, humic-like C1, and tryptophan-like C4. The $S_R$ also increased linearly with light absorption (Fig. 1c). Tyrosine-like C5 exhibited both increases and decreases with light absorption (Fig. 1f).

Photodegradation of DOM impacted its biodegradability, and the impacts differed among fractions of the DOM pool (Fig. 2). Photodegradation of humic-like C1 and tryptophan-like C4, those DOM fractions most strongly photodegraded, resulted in a 2.0-fold and 3.3-fold lower biodegradability on average compared to dark controls, respectively ($p < 0.001$; Table 3). Photodegradation resulted in a 10.1% ± 3.8% greater decrease of $S_R$ during biodegradation, on average, compared to dark controls ($p < 0.05$; Table 3). While photodegradation increased, decreased, or did not change subsequent biodegradation of $a_{305}$ and tyrosine-like C5 (Fig. 2), on average, there were no detectable changes in biodegradation of these fractions of DOM compared to dark controls (Table 3). On average, photodegradation increased the percentage of total BDOC by 2.5% ± 1.3% ($p < 0.001$; Table 3), ranging from a 9.1% ± 0.7% decrease to a 7.6% ± 3.0% increase (Fig. 2a). Photodegradation also increased the percentage of labile DOC by 3.5% ± 1.6% on average (Fig. 2a, triangles).

The extent of DOM photodegradation impacted subsequent differences in biodegradation of DOM in the light-exposed and dark control waters. The impacts differed among DOM fractions

**Table 3.** Average concentration of initial, photodegraded, and the total BDOM in WCC water. The percentage of DOM photodegraded or biodegraded is in parentheses. All values listed as average ± 1 SE.

| | | | Total BDOM ($n$ = 12) | |
|---|---|---|---|---|
| **DOM fraction** | **Initial DOM ($n$ = 5)** | **Photodegraded DOM ($n$ = 15)** | **Dark control** | **Light-exposed** |
| DOC (mg C $L^{-1}$) | 1.74 ± 0.17 | 0.08 ± 0.02 | 0.43 ± 0.02 | 0.46 ± 0.03 |
| | | (4.7 ± 1.1)* | (24.9 ± 0.6) | (27.4 ± 1.3)† |
| $a_{305}$ ($m^{-1}$) | 6.29 ± 0.80 | 1.36 ± 0.16 | 1.34 ± 0.14 | 1.09 ± 0.16 |
| | | (23.1 ± 2.9) | (20.8 ± 1.1) | (21.1 ± 1.2) |
| $SUVA_{254}$ (L mg $C^{-1}$ $m^{-1}$) | 2.74 ± 0.11 | 0.22 ± 0.04 | –0.20 ± 0.04 | –0.09 ± 0.02 |
| | | (8.0 ± 1.4) | (– 7.4 ± 1.5) | (– 4.0 ± 1.1) |
| $S_R$ | 0.70 ± 0.01 | –0.16 ± 0.02 | 0.05 ± 0.01 | 0.12 ± 0.03 |
| | | (– 22.8 ± 3.1)* | (6.4 ± 0.8) | (12.7 ± 2.8)† |
| Humic-like C1 (RU) | 0.47 ± 0.06 | 0.16 ± 0.01 | 0.08 ± 0.01 | 0.03 ± 0.01 |
| | | (36.2 ± 3.4)* | (16.9 ± 0.6) | (8.3 ± 1.6)† |
| Tryptophan-like C4 (RU) | 0.15 ± 0.02 | 0.05 ± 0.01 | 0.02 ± 0.01 | 0.01 ± 0.01 |
| | | (36.0 ± 3.3)* | (11.7 ± 0.9) | (3.5 ± 1.0)† |
| Tyrosine-like C5 (RU) | 0.06 ± 0.01 | 0.01 ± 0.01 | 0.03 ± 0.01 | 0.03 ± 0.01 |
| | | (3.5 ± 5.3)* | (55.1 ± 1.2) | (48.4 ± 7.7) |

*Significant differences between photodegraded DOM and total BDOM in the dark control (paired $t$-test, $p < 0.05$).
†Significant differences between total BDOM in the dark control and light-exposed waters (paired $t$-test, $p < 0.05$).

and were dependent upon the direction and magnitude of changes in the individual fractions during photodegradation (Fig. 3). For example, as humic-like C1 and tryptophan-like C4 were increasingly photodegraded, the biodegradability of these fractions generally decreased (Fig. 3). For humic-like C1, biodegradation decreased linearly with increasing photodegradation (Fig. 3d). As the extent of photodegradation increased, there was a greater decrease of $S_R$ during biodegradation compared to dark controls. That is, the light minus dark difference in decreased $S_R$ during biodegradation was proportional to the change in $S_R$ during photodegradation (Fig. 3c). When photodegradation produced ≥ 10% of tyrosine-like C5 (plotting below the origin on the $x$-axis), biodegradation of this component was enhanced. Conversely, when photodegradation removed ≥ 10% of tyrosine-like

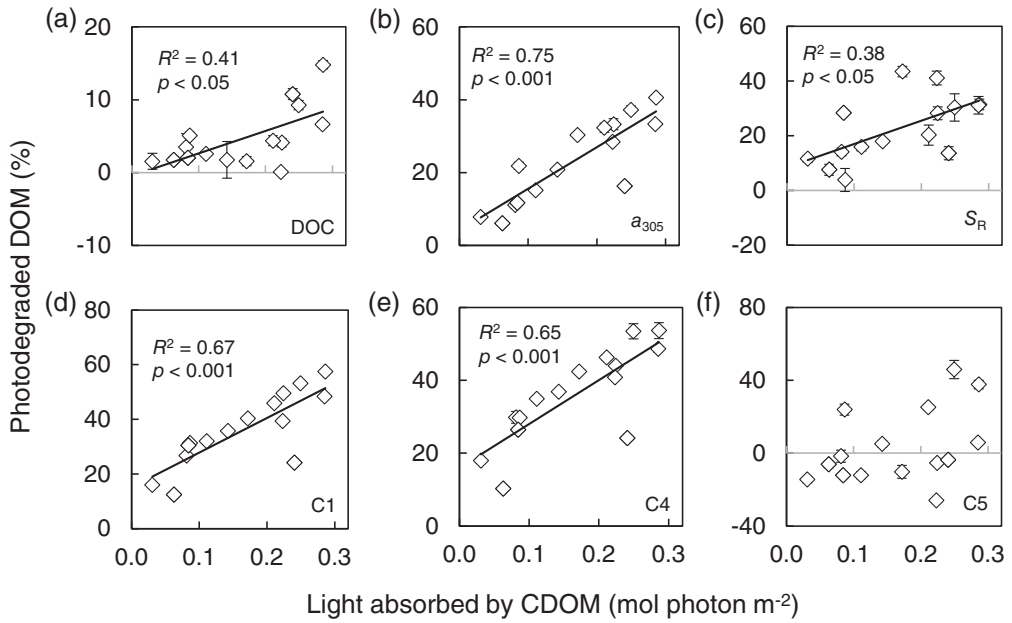


**Fig. 1.** Percentage of DOM photodegraded as a function of the amount of light absorbed by CDOM for: (a) DOC, (b) $a_{305}$, (c) $S_R$, (d) humic-like C1, (e) tryptophan-like C4, and (f) tyrosine-like C5. All values are average ± 1 SE of triplicate measurements.

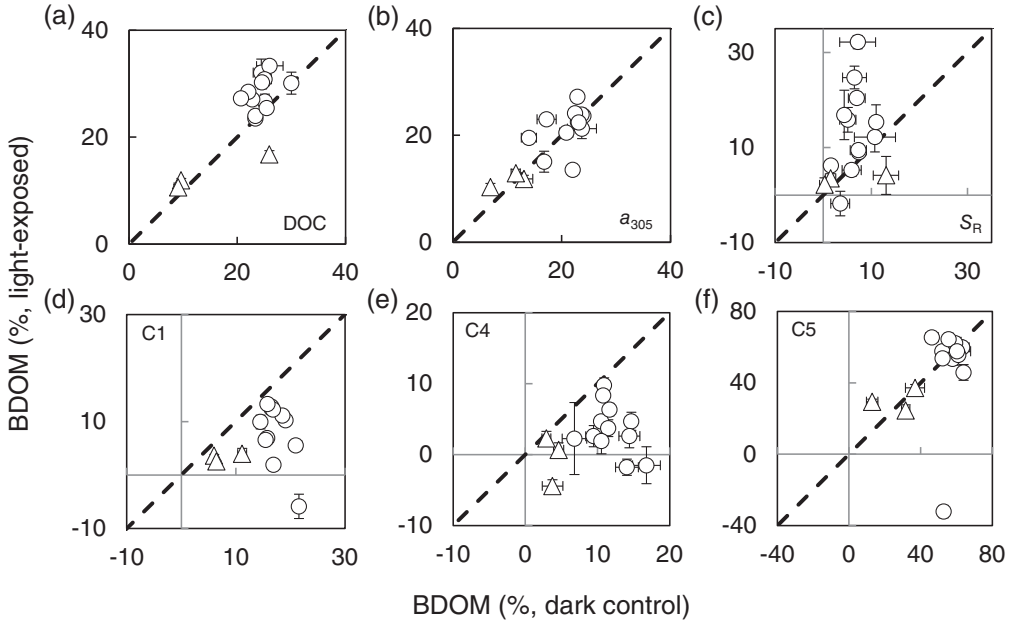


**Fig. 2.** Percentage of BDOM in the light-exposed vs. dark control waters plotted with the 1:1 line (dashed) for: (a) DOC, (b) $a_{305}$, (c) $S_R$, (d) humic-like C1, (e) tryptophan-like C4, and (f) tyrosine-like C5. Triangles indicate the labile pool within BDOM and circles indicate total BDOM. All data plotted as average ± 1 SE of triplicate measurements.

C5 (plotting above the origin on the *x*-axis), there was a lower biodegradability of this component on average (Fig. 3f). For $a_{305}$, there was either no impact of increasing photodegradation on subsequent biodegradation or an increase in biodegradation, until the highest extent of photodegradation, at which point biodegradation was diminished (Fig. 3b). After low levels of photodegradation (i.e., < 10% of DOC photomineralized), biodegradation of DOC generally increased, although in one of the stream waters, this was not the case. As the extent of photodegradation increased (i.e., > 10% of DOC photomineralized), no detectable changes in subsequent biodegradation were observed (Fig. 3a). Differences in the effect of photodegradation on the biodegradability of the total BDOC pool followed differences in the amount of light absorbed by

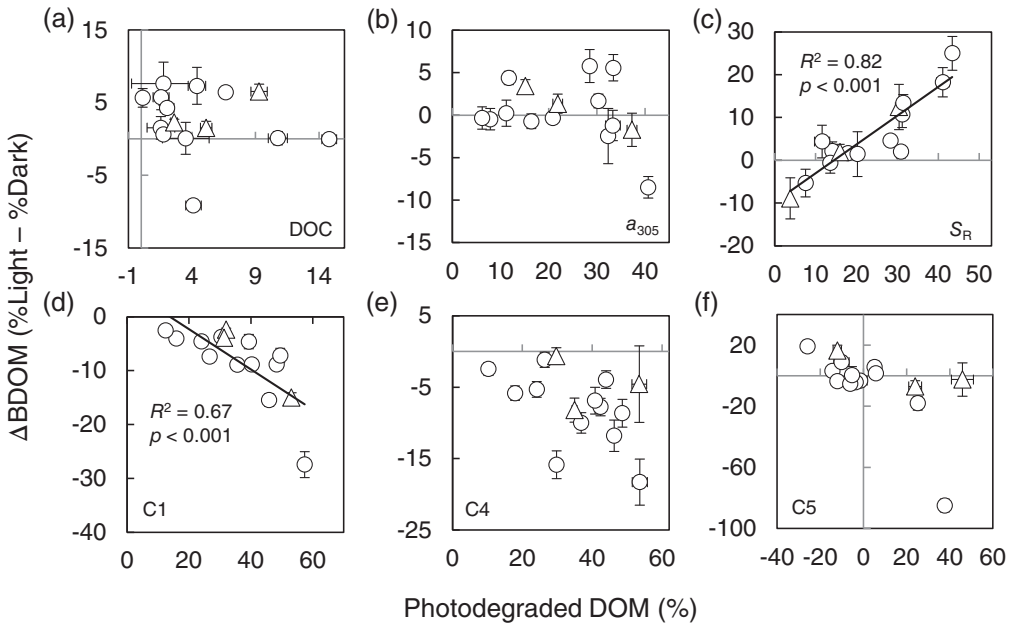


**Fig. 3.** Effect of photodegradation on BDOM vs. the percentage of DOM photodegraded for: (a) DOC, (b) $a_{305}$, (c) $S_R$, (d) humic-like C1, (e) tryptophan-like C4, and (f) tyrosine-like C5. Triangles indicate the labile pool within BDOM and circles indicate total BDOM. All data plotted as average ± 1 SE of triplicate measurements.

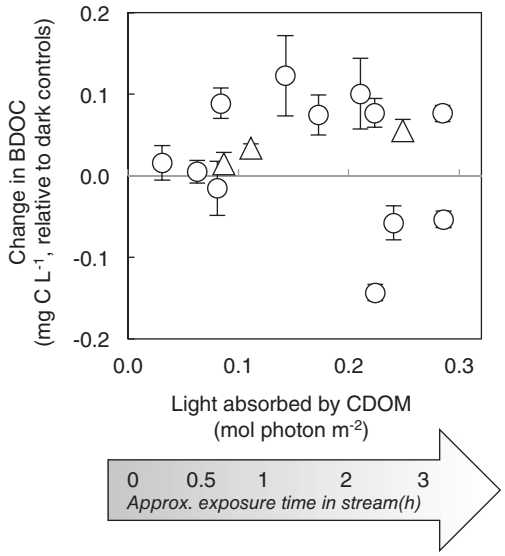


**Fig. 4.** Effect of photodegradation on BDOC concentration as a function of the amount of light absorbed by CDOM. Triangles indicate the labile pool within BDOC and circles indicate total BDOC. All data plotted as average ± 1 SE of triplicate measurements.

CDOM, where the one stream water which showed less biodegradation of total BDOC (Fig. 3a) experienced a higher amount of light absorbed by CDOM compared to most of the stream waters which showed enhanced biodegradation of total BDOC (Fig. 4).

The magnitude of DOM photodegradation rates compared to rates of biodegradation in WCC was strongly dependent upon the lability pool within BDOC. For labile DOC, rates of photomineralization, photochemical production, and photochemical removal in the water column were on average 22, 53, and 62 times slower, respectively, than rates of its biodegradation in the streambed of WCC (Table 4). In contrast, rates of photomineralization, photochemical production, and photochemical removal of semi-labile DOC were each about two times slower than the rates of its biodegradation in the streambed (Table 4). Thus, the sum of the rates of DOC photomineralization and photochemical alteration of semi-labile DOC overlapped with the average rate of biodegradation of semi-labile DOC in WCC (Table 4).

## Discussion

It is well established that photodegradation of terrestrially derived DOM can involve both photomineralization (Granéli et al. 1996; Lindell et al. 2000) and photo-alteration (Cory et al. 2007; Gonsoir et al. 2009; Ward and Cory 2016). Photomineralization removes carbon from the DOM pool, some of which may include BDOM. In contrast, photo-alteration can increase or decrease the BDOM pool by producing or removing biodegradable compounds, respectively, without reducing

**Table 4.** Areal rates of DOC biodegradation, photomineralization, photochemical production of BDOC, and photochemical removal of BDOC in WCC. All values listed as average ± 1 SE.

| Lability class | Areal rate of DOC biodegradation (mg C $m^{-2}$ $d^{-1}$) | Areal rate of photomineralization (mg C $m^{-2}$ $d^{-1}$) | Areal rate of photo-production of BDOC (mg C $m^{-2}$ $d^{-1}$) | | Areal rate of photo-removal of BDOC (mg C $m^{-2}$ $d^{-1}$) |
|---|---|---|---|---|---|
| | | | Calculated using a 1.5-min EBCT bioreactor | Calculated using a 37-min EBCT bioreactor | Calculated using a 37-min EBCT bioreactor |
| Labile | 304 ± 20 | — | 9 ± 1 | 8 ± 3 | 6 ± 2 |
| Semi-labile | 25 ± 1 | — | — | 13 ± 5 | 9 ± 3 |
| N/A | — | 16 ± 4 | — | — | — |

the size of the DOM pool (Wetzel et al. 1995; Cory et al. 2010*a*; Ward et al. 2017). Understanding what controls the balance between BDOM produced or removed by photomineralization and photo-alteration remains elusive, yet critical to assessing the impact of photodegradation on the biogeochemistry of DOM in stream ecosystems. Our research has provided new information concerning the overlap between fractions of DOM susceptible to both photo- and biodegradation as well as the role of photon dose in altering the balance between BDOM production and removal. Additionally, we have used that information to estimate the lowest amount of light needed to impact DOM biodegradability and generate the first quantitative comparison of rates of DOM photo- and biodegradation in a temperate headwater stream. These advances help reconcile disparate observations of both positive and negative effects of sunlight on DOM biodegradability and to improve our understanding of the role of photodegradation in the DOM biogeochemistry of stream ecosystems.

**Overlap between fractions of DOM photo- and biodegraded**

The large, significant changes in the biodegradability of DOC, CDOM, and FDOM following sunlight exposure (Fig. 2) provide strong evidence for the overlap between fractions of DOM degraded by sunlight and microbes. These findings extend prior work showing that the biodegradability of DOC, CDOM, and FDOM changes after photodegradation (Moran et al. 2000; Amado et al. 2007, 2015). Significant changes in the biodegradability of DOM following photodegradation are expected if sunlight competes with microbes by degrading the same fractions of DOM as microbes (Table 3). Changes in the biodegradability of DOC, CDOM, and FDOM after photodegradation could result from the loss of these fractions by photomineralization to $CO_2$. Following the photochemical loss of DOC, CDOM, and FDOM, lower concentrations of these fractions should be biodegraded because there was less of each fraction after sunlight exposure compared to dark controls (Table 3).

However, three lines of evidence suggest that photo-alteration, and not photomineralization, was primarily responsible for shifts in the biodegradability of DOM following photodegradation. First, there was only a small percentage of DOC photomineralized to $CO_2$ (on average 4.7% $\pm$ 1.1%; Table 3). Second, this loss of DOC by photomineralization did not result in a decrease in BDOC concentration of equal mass after photodegradation. For example, a greater mass of DOC was biodegraded in some of the light-exposed waters compared to dark controls (Fig. 4), despite less DOC available for microbes to degrade in light-exposed vs. dark control waters. This finding strongly suggests that the remaining, photo-altered DOM in these waters was more biodegradable than the dark control DOM. Similarly, for the stream waters that exhibited decreased biodegradability of DOM after photodegradation, a smaller mass of DOC was biodegraded in the light-exposed vs. dark control waters than the amount lost by photomineralization (Supporting Information Table S2). This finding suggests that, in these waters, the remaining, photo-altered DOM was less biodegradable than the dark control DOM. Third, photo-altered CDOM and FDOM differed in biodegradability compared to dark control CDOM and FDOM (Fig. 2). These results demonstrate that photo-alteration of DOM included both photo-production and photo-removal of different moieties within the BDOM pool.

For example, BDOM was likely photochemically produced during the breakdown of HMW, aromatic compounds to form LMW aromatics, as indicated from an increase in $S_R$ (Fig. 1c). These LMW, aromatic photo-products were more biodegradable than the HMW, aromatic DOM in the dark control (Fig. 3c). Many studies have shown that the molecular weight of terrestrially derived DOM decreases with increasing photodegradation (Helms et al. 2008; Gonsoir et al. 2013; Ward and Cory 2016), consistent with the fact that this DOM is comprised mostly of HMW, aromatic compounds (Kim et al. 2006; Cory et al. 2007; Sleighter et al. 2014; Ward and Cory 2015). BDOM may also be photochemically produced during the liberation of free amino acids from proteins within DOM (Jørgensen et al. 1998; Buffam and McGlathery 2003; Amado et al. 2015). Photochemical liberation of tyrosine may account for increased fluorescence of tyrosine-like FDOM after photodegradation in some instances (Fig. 1f). Increased biodegradability of tyrosine-like FDOM in proportion to its photochemical production (Fig. 3f) is consistent with higher biodegradability of free amino acids compared to those associated with proteins (Volk et al. 1997).

In contrast, lower biodegradability of the CDOM and FDOM remaining after photodegradation compared to dark controls (Fig. 2) indicated photochemical removal of BDOM. Decreased biodegradability of humic-like FDOM remaining after photodegradation compared to dark controls (Fig. 2d) is consistent with photo-oxidation of aromatic DOM to less biodegradable compounds compared to the parent compound (Cory et al. 2010*a*; Ward et al. 2017). Photo-alteration of tryptophan-like FDOM to oxidized amino acids (Pattison et al. 2012; Janssen et al. 2014), expected to be less biodegradable (Amado et al. 2007, 2015), is consistent with decreased biodegradability of this fraction of DOM compared to dark controls (Fig. 2e).

Although we cannot relate changes in the biodegradability of CDOM and FDOM (Fig. 3) to net changes in DOM biodegradability on a mass basis (Fig. 4), photo-alteration of HMW, aromatic DOM likely had a larger impact on the net change in BDOM than photo-alteration of amino acid-like DOM given that HWM, aromatic DOM accounts for more of the DOM pool on a mass basis compared to amino acid-like DOM. For example, HMW, aromatic compounds comprise at least 20% of terrestrially derived DOM (Cory et al. 2007; Hockaday et al. 2009), whereas nitrogen comprises less than 1% of terrestrially derived DOM by mass (Cory et al. 2007). Thus, photo-alteration of amino acid-like DOM constitutes an insufficient mass of carbon to account for net changes in BDOM. Given that photochemical production of acetate and other identifiable LMW acids or aldehydes accounts for at most ~ 20% of the increased BDOC concentration following photodegradation of

terrestrially derived DOM (Wetzel et al. 1995; Bertilsson and Tranvik 1998; Pullin et al. 2004), closing the mass balance on the net change in BDOM following photodegradation requires quantifying the fractions of LMW, aromatic DOM that contribute to the increased BDOC concentration (Cory et al. 2010*a*; Ward et al. 2017).

**BDOM changes with the amount of light absorbed by CDOM**

The impact of photodegradation on DOM biodegradability depended on the amount of light absorbed by CDOM because photochemical production and removal of BDOM varied with light absorption by CDOM (Fig. 4; as related to photon dose in Supporting Information Fig. S2). The net change in BDOM on a mass basis following photodegradation must result from the sum of photochemical production and removal of BDOM. For example, at the lowest amounts of light absorbed by CDOM (≤ 0.07 mol photon $m^{-2}$) when there was no significant difference in BDOC concentration between light-exposed and dark control waters (Fig. 4), photochemical production of BDOM was offset by removal of BDOM. As light absorption by CDOM increased in the range of 0.08–0.21 mol photon $m^{-2}$, the significant increases in BDOC concentration relative to dark controls (Fig. 4) suggest that photo-production of BDOM exceeded the removal of BDOM.

After CDOM absorbed higher amounts of light (≥ 0.22 mol photon $m^{-2}$), there was either an increase or a decrease in BDOC concentration relative to dark controls (Fig. 4). These large differences in the effect of photodegradation on BDOC concentrations after the same amount of light absorbed by CDOM (0.22 or 0.29 mol photon $m^{-2}$) may be in part due to differences in the extent of photomineralization of BDOM. For example, the stream waters that had decreased BDOC concentration after 0.22 or 0.29 mol photon $m^{-2}$ of light was absorbed by CDOM lost a greater mass of DOC by photomineralization than the stream waters that had increased BDOC concentration after the same amount of light was absorbed (Fig. 4; Supporting Information Table S2). These results suggest that with increasing loss of DOC by photomineralization, it is more likely that the loss includes BDOM, which can offset photo-production of BDOM.

Variability in the magnitude of increased BDOC concentration with light absorption by CDOM (i.e., photon dose) is consistent with prior work. Several studies have demonstrated smaller gains in microbial production or respiration after DOM received higher photon doses compared to lower photon doses (Wetzel et al. 1995; Reader and Miller 2014). This observation has been attributed in part to decreases in the yield of biodegradable photo-products with increasing photon dose (Biddanda and Cotner 2003; Cory et al. 2013, 2014; Reader and Miller 2014). For example, as HWM, aromatic DOM is increasingly altered by sunlight (Fig. 1b,c; Granéli et al. 1996; Lindell et al. 2000; Moran et al. 2000), there is less of this DOM to be converted to biodegradable LMW compounds (Biddanda and Cotner 2003). In addition, others have suggested that the smaller gains in microbial production or respiration after DOM received higher photon doses must also be due to photo-alteration of BDOM to compounds no longer biodegradable (Biddanda and Cotner 2003). Thus, the simultaneous photochemical production and removal of BDOM observed in our study help explain changes in the magnitude or direction of the effect of sunlight on DOM biodegradability.

**Photo- vs. biodegradation of DOM in the stream reach**

Photodegradation impacted DOM biodegradability in WCC water following sunlight exposure times that were comparable to hydraulic residence times in the stream reach. For example, we estimated that at least 30 min of sunlight exposure in unshaded reaches of WCC was needed to result in a change in BDOC concentration (Table 1; Fig. 4). Given that the stream water in this headwater reach of WCC is replaced by groundwater approximately every 9 to 13 h (in May and August, respectively; J. D. Newbold unpubl.) and, when the canopy is full (e.g., growing season), 16% and 14% of the reaches flow through semi-open canopy and meadows, respectively (Newbold et al. 1997), water column rates of light absorption by CDOM in WCC are fast enough for BDOM to be photochemically produced or removed. However, to impact organic matter processing in the stream reach, rates of DOM photodegradation would need to be comparable to rates of DOM biodegradation.

Similar rates of photo- and biodegradation of the semi-labile pool in WCC suggest substantial cooperation and competition between sunlight and microbes to degrade semi-labile DOM (Table 4). For example, rates of photodegradation of recalcitrant DOM to produce more semi-labile DOM or photochemical removal of semi-labile DOM are fast enough to increase or decrease the semi-labile pool, respectively, before being biodegraded several kilometers downstream. In contrast, the nearly 60 times slower rates of photo-production or photo-removal of labile DOC in the water column compared to rates of its biodegradation in the streambed suggest little interaction between sunlight and microbes to degrade labile DOM. That is, even if all fractions of DOM that are photo-altered or photomineralized comprise the labile pool, the rate of photodegradation of DOM in the water column would still be too slow to impact its biodegradation in the streambed.

An essential aspect of our research involved converting measures of photodegradation in quartz tubes into areal rates of DOM photodegradation representative of those in the stream. We accomplished this by selecting a range of sunlight exposure times that mimicked natural sunlight exposure times in the stream and quantifying all terms needed to relate experimental results to rates of photodegradation in the stream. Additionally, the stream waters used for sunlight exposure experiments were collected at sunrise so that the DOM would have had little to no prior exposure to sunlight. Our estimated rates of DOM photodegradation are representative of those in streams like WCC because there are no mixing limitations on DOM photodegradation rates in low turbidity waters where

CDOM is the main light-absorbing constituent in the water column and the rates of vertical mixing exceed rates of photodegradation in the water column (Li et al. 2019).

However, there remain large uncertainties bracketing our estimates of the areal rates of DOM photodegradation that call for caution in evaluating the comparisons between rates of photo- and biodegradation of DOM in streams and underscore the need for future studies to constrain these estimates. For example, areal rates of DOM photodegradation depend strongly on the wavelength dependence of the photochemical production and removal of BDOM, which are not known (*see* "Methods" section and Cory and Kling 2018). In addition, the areal rates of DOM photodegradation were obtained from experiments using stream water collected on only five dates and exposed to sunlight on mostly cloudy days. Thus, the rates of DOM light absorption in this study may represent a relatively narrow range of DOM photodegradation taking place in unshaded reaches of WCC. Rates of DOM photodegradation in streams like WCC also depend on the extent to which the reach is shaded from UV and visible sunlight. For example, rates of light absorption by CDOM, and thus DOM photodegradation, would be much lower in shaded compared to unshaded streams. Nonetheless, these first comparisons between rates of DOM photodegradation and biodegradation in a headwater stream tentatively suggest that photomineralization and photochemical alteration of the semi-labile pool may substantially impact the biogeochemistry of DOM in stream ecosystems.

## Conclusions and implications

This study demonstrated that just minutes of sunlight exposure in the stream can impact the biodegradability of DOM. The net effect of sunlight on DOM biodegradability changed with photon dose due to shifts in the balance of photochemical production and removal of BDOM. Overlap in the DOM fractions degraded by sunlight and microbes indicates that photo-alteration of DOM is relatively more important than photomineralization in the production and removal of BDOM. Given that water column rates of photochemical production and removal of semi-labile DOM were similar to rates of its biodegradation in the streambed, DOM photodegradation disproportionally impacts biodegradation of semi-labile DOM over labile DOM in streams.

In stream ecosystems, as the spatial scale expands from the headwaters to the catchment level, photodegradation of the semi-labile pool should play an increasingly important role in organic matter processing. Semi-labile and recalcitrant DOM largely escape biodegradation at the reach scale, with the semi-labile pool transported several kilometers downstream before it is biodegraded (Kaplan et al. 2008). Most streams increase in size with downstream distance, and based on hydrodynamics alone, biological uptake lengths should increase downstream as the product of increasing depth and velocity (Hall et al. 2013; McLaughlin and Kaplan 2013). Thus, in downstream reaches, there is greater likelihood that rates of photodegradation may equal or exceed rates of biodegradation of semi-labile DOM compared to upstream reaches. Furthermore, as semi-labile DOM is transported downstream, opportunities for photodegradation may increase in WCC, and streams in general, as shading from the riparian zone recedes to the edges of the widening channel and all of the available sunlight is absorbed by CDOM within the greater depth of water. Increasing export of terrestrially derived DOM to streams in response to changes in climate or land-use (Oni et al. 2015) could also increase rates of light absorption, and thus rates of photodegradation of DOM in streams.

## References


Amado, A. M., J. B. Cotner, A. L. Suhett, F. D. Assis Esteves, R. L. Bozelli, and V. F. Farjalla. 2007. Contrasting interactions mediate dissolved organic matter decomposition in tropical aquatic ecosystems. Aquat. Microb. Ecol. **49**: 25–34. doi:10.3354/ame01131

Amado, A. M., J. B. Cotner, R. M. Cory, B. L. Edhlund, and K. McNeill. 2015. Disentangling the interactions between photochemical and bacterial degradation of dissolved organic matter: Amino acids play a central role. Microb. Ecol. **69**: 554–566. doi:10.1007/s00248-014-0512-4

Battin, T. J., L. A. Kaplan, S. Findlay, C. S. Hopkinson, E. Marti, A. I. Packman, J. D. Newbold, and F. Sabater. 2008. Biophysical controls on organic carbon fluxes in fluvial networks. Nat. Geosci. **1**: 95–100. doi:10.1038/ngeo101

Bertilsson, S., and L. J. Tranvik. 1998. Photochemically produced carboxylic acids as substrates for freshwater bacterioplankton. Limnol. Oceanogr. **43**: 885–895. doi:10.4319/lo.1998.43.5.0885

Biddanda, B. A. 2017. Global significance of the changing freshwater carbon cycle. Eos **98**: 15–17. doi:10.1029/2017EO069751

Biddanda, B. A., and J. B. Cotner. 2003. Enhancement of dissolved organic matter bioavailability by sunlight and its role in the carbon cycle of Lakes Superior and Michigan. J. Great Lakes Res. **29**: 228–241. doi:10.1016/S0380-1330(03)70429-8

Buffam, I., and K. J. McGlathery. 2003. Effect of ultraviolet light on dissolved nitrogen transformations in coastal lagoon water. Limnol. Oceanogr. **48**: 723–734. doi:10.4319/lo.2003.48.2.0723

Coble, P. G. 1996. Characterization of marine and terrestrial DOM in seawater using excitation emission matrix spectroscopy. Mar. Chem. **51**: 325–346. doi:10.1016/0304-4203(95)00062-3

Cory, R. M., and D. M. McKnight. 2005. Fluorescence spectroscopy reveals ubiquitous presence of oxidized and reduced quinones in dissolved organic matter. Environ. Sci. Technol. **39**: 8142–8149. doi:10.1021/es0506962

Cory, R. M., D. M. McKnight, Y.-P. Chin, P. Miller, and C. L. Jaros. 2007. Chemical characteristics of fulvic acids from Arctic surface waters: Microbial contributions and photochemical transformations. J. Geophys. Res. **112**: G04S51. doi:10.1029/2006JG000343

Cory, R. M., K. McNeill, J. P. Cotner, A. Amado, J. M. Purcell, and A. G. Marshall. 2010*a*. Singlet oxygen in the coupled photo- and biochemical oxidation of dissolved organic matter. Environ. Sci. Technol. **44**: 3683–3689. doi:10.1021/es902989y

Cory, R. M., M. P. Miller, D. M. McKnight, J. J. Guerard, and P. L. Miller. 2010*b*. Effect of instrument-specific response on the analysis of fulvic acid fluorescence spectra. Limnol. Oceanogr.: Methods **8**: 67–78. doi:10.4319/lom.2010.8.0067

Cory, R. M., and L. A. Kaplan. 2012. Biological lability of streamwater fluorescent dissolved organic matter. Limnol. Oceanogr. **57**: 1347–1360. doi:10.4319/lo.2012.57.5.1347

Cory, R. M., B. C. Crump, J. A. Dobkowski, and G. W. Kling. 2013. Surface exposure to sunlight stimulates $CO_2$ release from permafrost soil carbon in the Arctic. Proc. Natl. Acad. Sci. USA **110**: 3429–3434. doi:10.1073/pnas.1214104110

Cory, R. M., C. P. Ward, B. C. Crump, and G. W. Kling. 2014. Sunlight controls water column processing of carbon in arctic fresh waters. Science **345**: 925–928. doi:10.1126/science.1253119

Cory, R. M., K. H. Harrold, B. T. Neilson, and G. W. Kling. 2015. Controls on dissolved organic matter (DOM) degradation in a headwater stream: The influence of photochemical and hydrological conditions in determining light-limitation or substrate limitation of photo-degradation. Biogeosciences **12**: 6669–6685. doi:10.5194/bg-12-6669-2015

Cory, R. M., and G. W. Kling. 2018. Interactions between sunlight and microorganisms influence dissolved organic matter degradation along the aquatic continuum. Limnol. Oceanogr.: Lett. **3**: 102–116. doi:10.1002/lol2.10060

Del Vecchio, R., and N. V. Blough. 2004. On the origin of the optical properties of humic substances. Environ. Sci. Technol. **38**: 3885–3891. doi:10.1021/es049912h

Fasching, C., and T. J. Battin. 2012. Exposure of dissolved organic matter to UV-radiation increases bacterial growth efficiency in a clear-water Alpine stream and its adjacent groundwater. Aquat. Sci. **74**: 143–153. doi:10.1007/s00027-011-0205-8

Gonsoir, M., B. M. Peake, W. T. Cooper, D. Podgorski, J. D'Andrilli, and W. J. Cooper. 2009. Photochemically induced changes in dissolved organic matter identified by ultrahigh resolution Fourier transform ion cyclotron resonance mass spectrometry. Environ. Sci. Technol. **43**: 698–703. doi:10.1021/es8022804

Gonsoir, M., P. Schmitt-Kopplin, and D. Bastviken. 2013. Depth-dependent molecular composition and photo-reactivity of dissolved organic matter in a boreal lake under winter and summer conditions. Biogeosciences **10**: 6945–6956. doi:10.5194/bg-10-6945-2013

Granéli, W., M. Lindell, and L. Tranvik. 1996. Photo-oxidative production of dissolved inorganic carbon in lakes of different humic content. Limnol. Oceanogr. **41**: 698–706. doi:10.4319/lo.1996.41.4.0698

Guillemette, F., and P. A. del Giorgio. 2011. Reconstructing the various facets of dissolved organic carbon bioavailability in freshwater ecosystems. Limnol. Oceanogr. **56**: 734–748. doi:10.4319/lo.2011.56.2.0734

Hall, R. O., M. A. Baker, E. J. Rosi-Marshall, J. L. Tank, and J. D. Newbold. 2013. Solute specific scaling of inorganic nitrogen and phosphorus uptake in streams. Biogeosciences **10**: 7323–7331. doi:10.5194/bg-10-7323-2013

Helms, J. R., A. Stubbins, J. D. Ritchie, E. C. Minor, D. J. Kieber, and K. Mopper. 2008. Absorption spectral slopes and slope ratios as indicators of molecular weight, source, and photobleaching of chromophoric dissolved organic matter. Limnol. Oceanogr. **53**: 955–969. doi:10.4319/lo.2008.53.3.0955

Hernes, P. J., B. A. Bergamaschi, R. S. Eckard, and R. G. M. Spencer. 2009. Fluorescence-based proxies for lignin in freshwater dissolved organic matter. J. Geophys. Res. **114**: G00F03. doi:10.1029/2009JG000938

Hockaday, W. C., J. M. Purcell, A. G. Marshall, J. A. Baldock, and P. G. Hatcher. 2009. Electrospray and photoionization mass spectrometry for the characterization of organic matter in natural waters: A qualitative assessment. Limnol. Oceanogr.: Methods **7**: 81–95. doi:10.4319/lom.2009.7.81

Janssen, E. M. -L., P. R. Erickson, and K. McNeill. 2014. Dual roles of dissolved organic matter as a sensitizer and quencher in the photooxidation of tryptophan. Environ. Sci. Technol. **48**: 4916–4924. doi:10.1021/es500535a

Jørgensen, N. O. G., L. Tranvik, H. Edling, W. Granéli, and M. Lindell. 1998. Effects of sunlight on occurrence and bacterial turnover of specific carbon and nitrogen compounds in lake waters. FEMS Microbol. Ecol. **25**: 217–227. doi:10.1111/j.1574-6941.1998.tb00474.x

Kaplan, L. A., and J. D. Newbold. 1995. Measurements of streamwater biodegradable dissolved organic carbon with a plug-flow bioreactor. Water Res. **29**: 2696–2706. doi:10.1016/0043-1354(95)00135-8

Kaplan, L. A., T. N. Wiegner, J. D. Newbold, P. H. Ostrom, and H. Gandhi. 2008. Untangling the complex issue of dissolved organic carbon uptake: A stable isotope approach. Freshw. Biol. **53**: 855–864. doi:10.1111/j.1365-2427.2007.01941.x

Kim, S., L. A. Kaplan, and P. G. Hatcher. 2006. Biodegradable dissolved organic matter in a temperate and a tropical stream determined from ultra-high resolution mass spectrometry. Limnol. Oceanogr. **51**: 1054–1063. doi:10.4319/lo.2006.51.2.1054

Laudon, H., J. Hedtjärn, J. Schelker, K. Bishop, R. Sørensen, and A. Ågren. 2009. Responses of dissolved organic carbon following forest harvesting in a boreal forest. Ambio **38**: 381–386. doi:10.1579/0044-7447-38.7.381

Li, A., A. F. Aubeneau, T. King, R. M. Cory, B. T. Neilson, D. Bolster, and A. I. Packman. 2019. Effects of vertical hydrodynamic mixing on photomineralization of dissolved organic carbon in arctic surface waters. Environ. Sci. Process. Impacts **21**: 748–760. doi:10.1039/c8em00455b

Lindell, M. J., H. W. Granéli, and S. Bertilsson. 2000. Seasonal photoreactivity of dissolved organic matter from lakes with contrasting humic content. Can. J. Fish. Aquat. Sci. **57**: 875–885. doi:10.1139/f00-016

McLaughlin, C., and L. A. Kaplan. 2013. Biological labilility of dissolved organic carbon in stream water and contributing terrestrial sources. Freshw. Sci. **32**: 1219–1230. doi:10.1899/12-202.1

Monteith, D. T., and others. 2007. Dissolved organic carbon trends resulting from changes in atmospheric deposition chemistry. Nature **450**: 537–540. doi:10.1038/nature06316

Moran, M. A., W. M. Sheldon, and R. G. Zepp. 2000. Carbon loss and optical property changes during long-term photochemical and biological degradation of estuarine dissolved organic matter. Limnol. Oceanogr. **45**: 1254–1264. doi:10.4319/lo.2000.45.6.1254

Murphy, K. R., C. A. Stedmon, T. D. Waite, and G. M. Ruiz. 2008. Distinguishing between terrestrial autochthonous organic matter sources in marine environments using fluorescence spectroscopy. Mar. Chem. **108**: 40–58. doi:10.1016/j.marchem.2007.10.003

Newbold, J. D., T. L. Bott, L. A. Kaplan, B. W. Sweeney, and R. L. Vannote. 1997. Organic matter dynamics in White Clay Creek, Pennsylvania, USA. J. North Am. Benthol. Soc. **16**: 46–50. doi:10.2307/1468231

Obernosterer, I., and R. Benner. 2004. Competition between biological and photochemical processes in the mineralization of dissolved organic carbon. Limnol. Oceanogr. **49**: 117–124. doi:10.4319/lo.2004.49.1.0117

Oni, S. K., T. Tiwari, J. L. J. Ledesma, A. M. Ågren, C. Teutschbein, J. Schelker, H. Laudon, and M. N. Futter. 2015. Local- and landscape-scale impacts of clear-cuts and climate change on surface water dissolved organic carbon in boreal forests. Eur. J. Vasc. Endovasc. Surg. **120**: 2402–2426. doi:10.1002/2015JG003190

Pattison, D. I., A. S. Rahmanto, and M. J. Davies. 2012. Photo-oxidation of proteins. Photochem. Photobiol. Sci. **11**: 38–53. doi:10.1039/C1PP05164D

Pullin, M. J., S. Bertilsson, J. V. Goldstone, and B. M. Voelker. 2004. Effects of sunlight and hydroxyl radical on dissolved organic matter: Bacterial growth efficiency and production of carboxylic acids and other substrates. Limnol. Oceanogr. **49**: 2011–2022. doi:10.4319/lo.2004.49.6.2011

Reader, H. E., and W. L. Miller. 2014. The efficiency and spectral photon dose dependence of photochemically induced changes to the bioavailability of dissolved organic carbon. Limnol. Oceanogr. **59**: 182–194. doi:10.4319/lo.2014.59.1.0182

Singh, N. K., W. M. Reyes, E. S. Bernhardt, R. Bhattacharya, J. L. Meyer, J. D. Knoepp, and R. E. Emanuel. 2016. Hydro-climatological influences on long-term dissolved organic carbon in a mountain stream of the southeastern United States. J. Environ. Qual. **45**: 1286–1295. doi:10.2134/jeq2015.10.0537

Sleighter, R. L., R. M. Cory, L. A. Kaplan, H. A. N. Abdulla, and P. G. Hatcher. 2014. A coupled geochemical and biogeochemical approach to characterize the bioreactivity of dissolved organic matter from a headwater stream. Eur. J. Vasc. Endovasc. Surg. **199**: 1520–1537. doi:10.1002/2013JG002600

Stedmon, C. A., and S. Markager. 2005. Tracing the production and degradation of autochthonous fractions of dissolved organic matter by fluoresence analysis. Limnol. Oceanogr. **50**: 1415–1426. doi:10.4319/lo.2005.50.5.1415

Stedmon, C. A., and R. Bro. 2008. Characterizing dissolved organic matter fluorescence with parallel factor analysis: A tutorial. Limnol. Oceanogr.: Methods **6**: 572–579. doi:10.4319/lom.2008.6.572

Tranvik, L. J., and S. Bertilsson. 2001. Contrasting effects of solar UV radiation on dissolved organic sources for bacterial growth. Ecol. Lett. **4**: 458–463. doi:10.1046/j.1461-0248.2001.00245.x

Tyndall, J. 1877. On heat as a germicide when discontinuously applied. Proc. R. Soc. Lond. **25**: 569–570. doi:10.1098/rspl.1876.0090

Vähätalo, A. V., M. Salkinoja-Salonen, P. Taalas, and K. Salonen. 2000. Spectrum of the quantum yield for photochemical mineralization of dissolved organic carbon in a humic lake. Limnol. Oceanogr. **45**: 664–676. doi:10.4319/lo.2000.45.3.0664

Volk, C. J., C. B. Volk, and L. A. Kaplan. 1997. Chemical composition of biodegradable dissolved organic matter in streamwater. Limnol. Oceanogr. **42**: 39–44. doi:10.4319/lo.1997.42.1.0039

Ward, C. P., and R. M. Cory. 2015. Chemical composition of dissolved organic matter draining permafrost soils. Geochim. Cosmochim. Acta **167**: 63–79. doi:10.1016/j.gca.2015.07.001

Ward, C. P., and R. M. Cory. 2016. Complete and partial photo-oxidation of dissolved organic matter draining permafrost soils. Environ. Sci. Technol. **50**: 3545–3553. doi:10.1021/acs.est.5b05354

Ward, C. P., S. G. Nalven, B. C. Crump, G. W. Kling, and R. M. Cory. 2017. Photochemical alteration of organic carbon draining permafrost soils shifts microbial metabolic pathways and stimulates respiration. Nat. Commun. **8**: 772. doi:10.1038/s41467-017-00759-2

Weishaar, J. L., G. R. Aiken, B. A. Bergamaschi, M. S. Fram, R. Fujii, and K. Mopper. 2003. Evaluation of specific ultraviolet absorbance as an indicator of the chemical composition and reactivity of dissolved organic carbon. Environ. Sci. Technol. **37**: 4702–4708. doi:10.1021/es030360x

Wetzel, R. G., P. G. Hatcher, and T. S. Bianchi. 1995. Natural photolysis by ultraviolet irradiance of recalcitrant dissolved organic matter to simple substrates for rapid bacterial metabolism. Limnol. Oceanogr. **40**: 1369–1380. doi:10.4319/lo.1995.40.8.1369

## Acknowledgments

We thank Michael D. Gentile, Sherman L. Roberts, and Lija A. Treibergs for assistance with field and laboratory work. Support for this work came from NSF grants EAR-1451372 to RMC, EAR-1452039 to LAK, and the Scott Turner Research Award in Earth Sciences at the University of Michigan to JCB.

## Conflict of Interest

None declared.

*Submitted 21 January 2019*
*Revised 11 May 2019*
*Accepted 04 June 2019*

*Associate editor: John Melack*